AIP | Applied Physics Letters

Nanoscale fluctuations on epithelial cell surfaces investigated by scanning ion conductance microscopy

Yusuke Mizutani, Myung-Hoon Choi, Sang-Joon Cho, and Takaharu Okajima

Citation: Appl. Phys. Lett. **102**, 173703 (2013); doi: 10.1063/1.4803469
View online: http://dx.doi.org/10.1063/1.4803469
View Table of Contents: http://apl.aip.org/resource/1/APPLAB/v102/i17
Published by the AIP Publishing LLC.

Nanoscale fluctuations on epithelial cell surfaces investigated by scanning ion conductance microscopy

Yusuke Mizutani,[1] Myung-Hoon Choi,[2] Sang-Joon Cho,[2,3] and Takaharu Okajima[1,a)]
[1]*Graduate School of Information Science and Technology, Hokkaido University, Kita-ku N14 W9, Sapporo 060-0814, Japan*
[2]*Park Systems Inc., Suwon 443-270, Republic of Korea*
[3]*Advanced Institute of Convergence Technology, Seoul National University, Suwon 443-270, Republic of Korea*

(Received 16 February 2013; accepted 15 April 2013; published online 30 April 2013)

Nanoscale fluctuations on the apical surfaces of epithelial cells connected to neighboring cells were investigated by scanning ion conductance microscopy. Mapping the ion current as a function of the tip–surface distance revealed that in untreated cells, the apparent fluctuation amplitude increased towards the cell center. We found that the spatial dependence was less correlated with the heterogeneities of cell stiffness but was significantly reduced when actin filaments were disrupted. The results indicate that apical surface fluctuations are highly constrained at the cell–cell interface, in the vertical direction to the surface and by the underlying actin filaments. © *2013 AIP Publishing LLC*. [http://dx.doi.org/10.1063/1.4803469]

Membranes are essential components of all cells. Because cell membranes are flexible and undergo dynamic morphological changes according to biological functions, the characterization of cell surface fluctuations is crucial for a better understanding of cell function in relation to cell dynamics. Red blood cells have been extensively used as a model for investigating cell surface fluctuations because they lack nuclei and consist of a lipid bilayer coupled to a regular two-dimensional cytoskeletal network that is regarded as an optically isotropic material. Sophisticated optical techniques that detect phase differences in light transmitted through the cytoplasm of cells revealed that the fluctuation between the upper and lower surfaces in the single cells exhibited a spatial dependence with an amplitude of tens of nanometers[1–4] that was mediated by the underlying cytoskeleton.[1–6]

Compared with non-adherent cells such as red blood cells, adherent mammalian cells have more heterogeneous surface structures. In multicellular epithelial cell sheets, the cells adhere to the extracellular matrix via their basal surface and are coupled to neighboring cells at the cell–cell interface (lateral surfaces). Thus, epithelial cell surfaces are classified into apical, lateral, and basal surfaces. Recent studies have unveiled the detailed dynamic properties of the basal and lateral surfaces.[7–10] However, less is known about the fluctuations of apical cell surfaces, as observed in red blood cells, which are also vital for the activation of various signaling pathways during cell communication.

Optical techniques have been applied to estimate the vertical height of adherent mammalian cells.[11–13] However, the optical refractive index of the cells may fluctuate according to the remodeling of the intracellular cytoskeletal network and/or the displacement of subcellular organelles. Thus, non-optical techniques for directly measuring flexible cell surface positions are required to quantify nanoscale fluctuations on adherent cell surfaces.

Scanning ion conductance microscopy (SICM)[14] is a promising tool for analyzing local regions on cell surfaces[15–18] through an ion current, I, that flows through the small bore of a pipette. Using SICM, Gorelik *et al.*[16] reported the direct observation of the dynamic formation and assembly of microvilli on apical epithelial cell surfaces at high resolution without substantial cell deformation. This result indicates that the change in I observed in live epithelial cells is highly dependent on the tip–surface distance, D. In this letter, we characterize I-D curves on epithelial Mardin-Darby canine kidney (MDCK) cell sheets in which the cells were almost fully confluent and translational cell migration was highly constrained, and estimate the nanoscale fluctuations on the apical cell surfaces from the observed I-D curves.

We used a commercial SICM (XE-Bio, Park Systems) with a nanopipette of ca. 100 nm inner diameter (Fig. S1 in supplementary material[20]). Images of live MDCK cell sheets were obtained in the so-called hopping mode,[17] also referred to as approach-retract scanning (ARS) mode,[19] in which each I-D curve was measured for ca.10 ms (Fig. 1(a)). As shown in Fig. 1(b), the cross-sectional topography of MDCK cell surfaces whose height increased around the cell center was clearly imaged in this mode. For I-D curve measurements, we measured fifty I-D curves at each position on the cell surface at the same scan speed as the hopping/ARS mode imaging. The measured I-D curves were averaged to characterize the I-D curve at different positions on the cell surface. The mechanical properties of the cells at different positions were measured by atomic force microscopy (AFM). To investigate the effects of actin filaments and microtubules on the I-D curves and the cells' mechanical properties, the cells were incubated with latrunculin-A (latA) (0.5 μM, Sigma-Aldrich) or colchicine (col) (50 μM, Sigma-Aldrich) for 30 min before the measurements. Further details regarding the experimental methods can be found in the supplementary material.[20]

Figure 1(c) shows I-D curves measured at a position around the center of cells prepared with different treatments. We observed four different types of I-D curves. First, the I-D

a)Author to whom correspondence should be addressed. Electronic mail: okajima@ist.hokudai.ac.jp

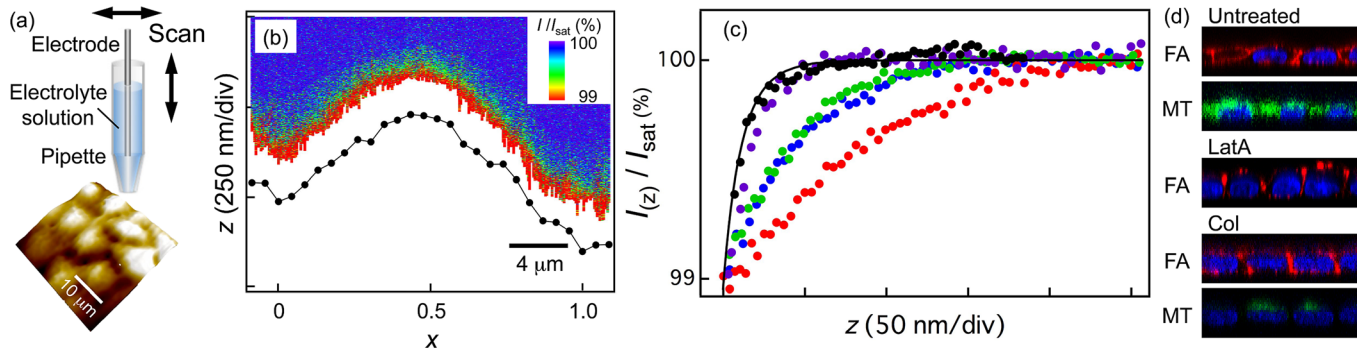

FIG. 1. (a) SICM image (40 μm × 40 μm) of MDCK cells in an epithelial sheet. (b) A set of non-averaged ion current–distance curves measured in one dimension over a cell around the cell center. The black dots represent averaged z_0 estimated from Eq. (3). (c) *I-D* curves measured in a solid substrate (black) and in fixed (purple), untreated (blue), col-treated (green), and latA-treated (red) cells. The curves are plotted such that the z positions are identical at a 1% reduction in the ion current. The solid line represents the solid substrate fitted to Eq. (3). (d) Cross-sectional confocal microscopic images of actin filaments (FA) and microtubules (MT) in untreated cells (untreated), cells treated with latA (LatA), and cells treated with col (Col) in the epithelial sheet.

curve obtained in chemically fixed cells was similar to that in solid substrates composed of silicon and solid rubber materials (Fig. S2 in supplementary material[20]). Second, the *I-D* curve in untreated (un-fixed) cells was much broader compared with the chemically fixed cells. Third, the broadness remained unchanged in cells whose microtubules were disrupted by col (Fig. 1(d)). Fourth, the disruption of actin filaments by latA (Fig. 1(d)) significantly enhanced the broadness of the curve.

The measurement time for the single *I-D* curve shown in Fig. 1(c) was less than one second, which corresponds to a few nm of dynamic morphological changes such as microvilli on the epithelial cell surface.[16] Indeed, it was confirmed that the profile of the *I-D* curve was almost unchanged during the measurement timeframe (Fig. S3 in supplementary material[20]). This indicates that the broadness of the *I-D* curves shown in Fig. 1(c) is not associated with dynamic morphological changes. Moreover, we found no significant correlation between the profile of *I-D* curves and the local topographical variation (Fig. S4 in supplementary material[20]) measured in the hopping/ARS mode. Therefore, we consider that the observed *I-D* curves reflect cell surface fluctuations, which appear in regions larger than those that can be resolved by SICM imaging.

To estimate the cell surface fluctuations from the *I-D* curves, we propose the model schematically described in Fig. 2(a). The cell surface position, $z_s(x, t)$, at time t at a normalized lateral position x is generally defined as $z_s(x, t) = z_0(x) + \delta z_s(x, t)$. $z_0(x)$ is the average z-position of the apical cell surface, and $\delta z_s(x, t)$ is the fluctuation of the z position around $z_0(x)$, i.e., $\langle \delta z_s(x) \rangle = 0$, where the bracket $\langle X \rangle$ represents the ensemble or time average of the quantity X. Here, we assume that the cell surfaces fluctuated with a Gaussian stochastic distribution, P, with the root mean square (RMS) displacement of surface fluctuations, $\langle \delta z_s^2 \rangle^{1/2}$, which is the apparent amplitude of cell surface fluctuation, as given by

$$P(z_s - z_0,\ \langle \delta z_s^2 \rangle) = \frac{1}{\sqrt{2\pi \langle \delta z_s^2 \rangle}} \exp\{-(z_s - z_0)^2 / (2\langle \delta z_s^2 \rangle)\}. \tag{1}$$

The *I-D* curve in the solid substrate without fluctuation was well fitted to Eq. (2)[21] (Fig. 1(c))

$$I_0(z - z_0) = I_{sat}\left[1 + \frac{\zeta}{z - z_0}\right]^{-1}, \tag{2}$$

where z is the tip position, z_0 is sample surface position with no fluctuations, I_{sat} is the ion current when the pipette is far from the sample surface, and ζ is a function of the inner radius of the tip opening, the inner radius of the tip base, the tip length, and the conductivity of an electrolyte (in this case, serum-free culture medium) in the pipette.[21] It was

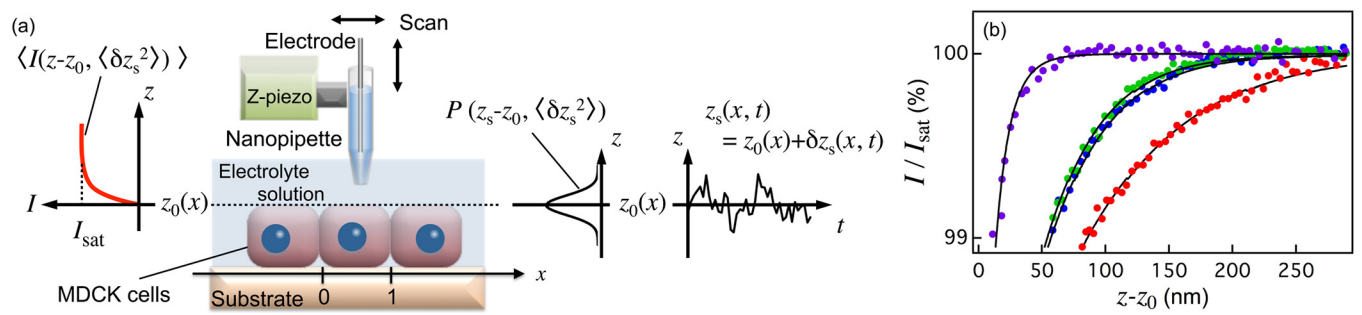

FIG. 2. (a) Schematic illustration of the measurement of apical cell surface fluctuations by SICM. The apical cell surfaces fluctuate with δz_s (x, t) around $z = z_0(x)$ at a normalized lateral position x (0 and 1 at the cell edge and 1/2 at the cell center) at time t. The apical cell surface position is statistically expressed as a Gaussian stochastic distribution, P, with the RMS displacement of surface fluctuations, which is the apparent amplitude of cell surface fluctuation. Then, $\langle I \rangle$ consequently follows Eq. (3). (b) *I-D* curves of fixed (purple), untreated cells (blue), latA-treated cells (red) and col-treated cells (green). The solid lines show the results fitted to Eq. (3).

experimentally determined ζ to be 4.9×10^{-2} nm for an I_{sat} of ~950 pA in the culture medium (Fig. S2 in supplementary material[20]). Thus, when the cell fluctuations follow Eq. (1), the averaged I, $\langle I \rangle$, measured at z on cells at z_0 with $\langle \delta z_s^2 \rangle^{1/2}$, is expressed as

$$\langle I(z - z_0,\ \langle \delta z_s^2 \rangle) \rangle = \int_{-\infty}^{\infty} I_0(z - z_s) P(z_s - z_0,\ \langle \delta z_s^2 \rangle) dz_s, \tag{3}$$

where z_0 and $\langle \delta z_s^2 \rangle$ are fitting parameters. It is noted that the dynamic range of the cell surface fluctuations that we can observe in this study is restricted from several Hz, which depends on the measurement time of *I-D* curve, to 1.1 kHz, which is the bandwidth of the preamplifier of the SICM instrument.

The *I-D* curves shown in Fig. 1(c) were well fitted to Eq. (3) (Fig. 2(b)). In the fixed cells, the RMS displacement of surface fluctuations was estimated to be 6.5 nm, which is consistent with that in fixed red blood cells by optical techniques.[4] The displacements increased significantly to be ca. 60 nm in the untreated and col-treated cells and ca. 105 nm in the latA-treated cells, although the treatment caused no significant difference in apical cell topography (Fig. S5 in supplementary material[20]).

Figure 3 shows the RMS displacement of surface fluctuations estimated at different positions on the cell surface. Interestingly, in the untreated cells, the cell surface fluctuation exhibited a clear spatial-dependence that increased towards the cell center, i.e., the RMS displacement of surface fluctuations was 46 nm at the cell edge and 71 nm at the cell center, whereas no spatial dependence was observed in the fixed cells. Moreover, in the latA-treated cells, the spatial dependence was significantly reduced. This result indicates that

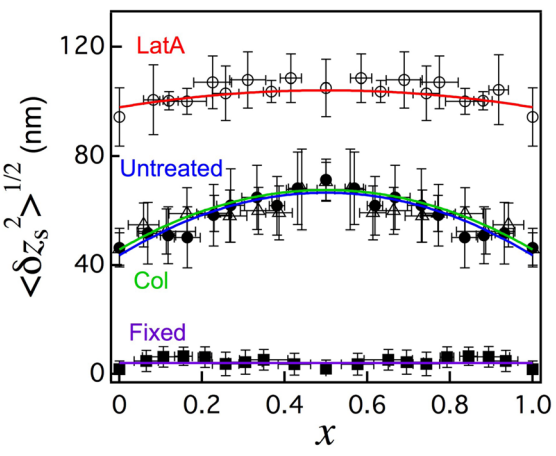

FIG. 3. RMS displacements of surface fluctuations, which is defined in Eq. (1), of fixed cells ($N = 6$) (purple line), untreated cells ($N = 18$) (blue line), col-treated cells ($N = 11$) (green line), and latA-treated cells ($N = 12$) (red line), measured in lines crossing over the center of the cells by SICM. The data were approximately fitted as a parabolic shape. Note that the displacements are less than 10 nm on a fixed cell surface but much larger and have a spatial dependence on unfixed cell surfaces. The fluctuations are largest on latA-treated cell surfaces suggesting that when the actin filamentous network inside the cell is disrupted the fluctuations become larger. By contrast, the fluctuations do not increase, and the spatial dependence remains unchanged when the microtubules are disrupted by col.

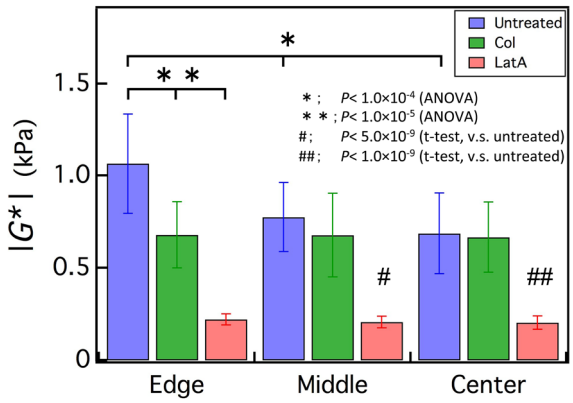

FIG. 4. Magnitude of shear modulus, $|G^*|$, at 100 Hz in untreated cells ($N = 11$) (blue), latA-treated cells ($N = 11$) (red), and col-treated cells ($N = 11$) (green) at different intracellular regions, including the cell edge, the cell center, and the middle position, which was between the cell edge and the cell center of single MDCK cells.

the spatial heterogeneities in epithelial cell surface fluctuations are strongly associated with the underlying actin cytoskeleton. Col-treated cells remained unchanged in both the spatial-dependence and the magnitude of the displacement of surface fluctuations, indicating that the fluctuations on the apical cell surface are less affected by microtubules.

Because the modification of cytoskeletal structures influences the mechanical properties of cells,[22] we investigated the relationship between the cells' mechanical properties and the estimated fluctuations on the cell surface. Figure 4 shows the magnitude of shear modulus, $|G^*|$ at a frequency of 100 Hz, determined in cells at different cell positions by AFM. It was observed that in untreated cells, the cell edge was stiffer than the cell center. Importantly, as the cells were treated with col, $|G^*|$ at the cell edge significantly decreased and attained the same value as that measured in other regions. This result indicates that microtubules stabilize the cellular structures at the cell edge.[23–25]

It was reported[26,27] that hydrostatic forces applied to the sample surface through the SICM tip deformed soft cell surfaces, and consequently the resultant *I-D* curve profiles were different to those on solid substrates. We found that the col-treated cells became mechanically homogeneous (Fig. 4). This indicates that the spatial dependence of *I-D* curves measured in the col-treated cells was dominated by the cell surface fluctuations, but not the hydrostatic forces. Thus, the mechanical properties of the cells are not directly correlated with cell surface fluctuations.

By contrast, the disruption of actin filaments caused a significant reduction in $|G^*|$ across all regions, indicating that actin filaments play a primary role in maintaining cell stiffness. Similar to the col-treated cells, the latA-treated cells were mechanically homogeneous but became very soft. The latA-treated cells are likely sensitive to the hydrostatic force, and the RMS displacement of surface fluctuations estimated by Eq. (3) (Figs. 2(b) and 3) might be overestimated. However, because the mechanical properties of latA-treated cells have no spatial dependence (Fig. 4), the observed reduction of the spatial dependence in latA-treated cells (Fig. 3) is not dependent on the hydrostatic forces. These results strongly suggest that the lateral surfaces are highly

constrained in the vertical direction to the apical cell surface by the underlying actin filaments. It is known that the actin filaments strongly interact with the adherens junctions that connect the cells.[25,28] The effect of this pinning, which is associated with the formation of actin filaments, may dominate the spatial heterogeneities of the epithelial cell surface fluctuations.

In summary, we characterized the *I-D* curves on epithelial cell sheets measured by SICM and estimated the nanoscale fluctuations in the apical cell surfaces from the observed *I-D* curves using a simple model. Regarding cell surface fluctuations measured by other direct methods, Pelling *et al.*[29] showed that AFM can measure local temperature-dependent nanomechanical motion in the yeast cell wall. However, because mammalian cells are much softer than yeast cells, the AFM tip may perturb mammalian cell surfaces.[30] Thus, the SICM method presented here is a unique non-contact scanning probe microscopy technique for quantifying the apparent fluctuation amplitude of adherent epithelial cell surfaces.

We thank M. Suzuki and H. Tokumoto for helpful discussion and Z. Ishikura for technical assistance. This study was supported in part by Grant-in-Aid for Challenging Exploratory Research (23656055), Grant-in-Aid for Scientific Research on Innovative Areas "Bio-assembler"(24106501), the Global-COE Program "Center for Next-Generation Information Technology based on Knowledge Discovery and Knowledge Federation" from the Ministry of Education, Culture, Sports, Science and Technology (MEXT) of Japan (T.O), and the Industrial Source Technology Development Program (ISTDP 10033633 to S.J.C.) of the Ministry of Knowledge Economy of Korea. Instrument development was also sponsored by the Industrial Source Technology development Program (ISTDP 10033633 to S.J.C) in Ministry of Knowledge Economy in Korea.

[1]G. Popescu, Y. Park, W. Choi, R. R. Dasari, M. S. Feld, and K. Badizadegan, Blood Cells Mol. Dis. **41**, 10 (2008).
[2]Y. K. Park, M. Diez-Silva, G. Popescu, G. Lykotrafitis, W. S. Choi, M. S. Feld, and S. Suresh, Proc. Natl. Acad. Sci. U.S.A. **105**, 13730 (2008).
[3]Y. K. Park, C. A. Best, T. Auth, N. S. Gov, S. A. Safran, G. Popescu, S. Suresh, and M. S. Feld, Proc. Natl. Acad. Sci. U.S.A. **107**, 1289 (2010).
[4]B. Rappaz, A. Barbul, A. Hoffmann, D. Boss, R. Korenstein, C. Depeursinge, P. J. Magistretti, and P. Marquet, Blood Cells Mol. Dis. **42**, 228 (2009).
[5]N. S. Gov and S. A. Safran, Biophys. J. **88**, 1859 (2005).
[6]R. Shlomovitz and N. S. Gov, Phys. Rev. Lett. **98**, 168103 (2007).
[7]J. Kaefer, Proc. Natl. Acad. Sci. U.S.A. **104**, 18549 (2007).
[8]M. Rauzi, P. Verant, T. Lecuit, and P.-F. Lenne, Nat. Cell Biol. **10**, 1401 (2008).
[9]V. Maruthamuthu, B. Sabass, U. S. Schwarz, and M. L. Gardel, Proc. Natl. Acad. Sci. U.S.A. **108**, 4708 (2011).
[10]Q. Tseng, E. Duchemin-Pelletier, A. Deshiere, M. Balland, H. Guillou, O. Filhol, and M. Thery, Proc. Natl. Acad. Sci. U.S.A. **109**, 1506 (2012).
[11]J. Reed, J. J. Troke, J. Schmit, S. Han, M. A. Teitell, and J. K. Gimzewski, ACS Nano **2**, 841 (2008).
[12]J. Reed, J. Chun, T. A. Zangle, S. Kalim, J. S. Hong, S. E. Pefley, X. Zheng, J. K. Gimzewski, and M. A. Teitell, Biophys. J. **101**, 1025 (2011).
[13]T. Yamauchi, H. Iwai, and Y. Yamashita, Opt. Express **19**, 5536 (2011).
[14]P. K. Hansma, B. Drake, O. Marti, S. A. C. Gould, and C. B. Prater, Science **243**, 641 (1989).
[15]Y. E. Korchev, C. L. Bashford, M. Milovanovic, I. Vodyanoy, and M. J. Lab, Biophys. J. **73**, 653 (1997).
[16]J. Gorelik, A. I. Shevchuk, G. I. Frolenkov, I. A. Diakonov, M. J. Lab, C. J. Kros, G. P. Richardson, I. Vodyanoy, C. R. W. Edwards, D. Klenerman, and Y. E. Korchev, Proc. Natl. Acad. Sci. U.S.A. **100**, 5819 (2003).
[17]P. Novak, C. Li, A. I. Shevchuk, R. Stepanyan, M. Caldwell, S. Hughes, T. G. Smart, J. Gorelik, V. P. Ostanin, M. J. Lab, G. W. J. Moss, G. I. Frolenkov, D. Klenerman, and Y. E. Korchev, Nat. Methods **6**, 279 (2009).
[18]J. Rheinlaender, N. A. Geisse, R. Proksch, and T. E. Schäffer, Langmuir **27**, 697 (2011).
[19]F. Anariba, J. H. Anh, G.-E. Jung, N.-J. Cho, and S.-J. Cho, Mod. Phys. Lett. B **26**, 1130003 (2012).
[20]See supplementary material at http://dx.doi.org/10.1063/1.4803469 for further details on our experimental materials and methods.
[21]H. Nitz, J. Kamp, and H. Fuchs, Probe Microsc. **1**, 187 (1998).
[22]C. Rotsch and M. Radmacher, Biophys. J. **78**, 520 (2000).
[23]W. Meng, Y. Mushika, T. Ichii, and M. Takeichi, Cell **135**, 948 (2008).
[24]S. J. Stehbens, A. D. Paterson, M. S. Crampton, A. M. Shewan, C. Ferguson, A. Akhmanova, R. G. Parton, and A. S. Yap, J. Cell Sci. **119**, 1801 (2006).
[25]R. M. Mege, J. Gavard, and M. Lambert, Curr. Opin. Cell Biol. **18**, 541 (2006).
[26]M. Pellegrino, P. Orsini, M. Pellegrini, P. Baschieri, F. Dinelli, D. Petracchi, E. Tognoni, and C. Ascoli, Neurosci. Res. **69**, 234 (2011).
[27]M. Pellegrino, M. Pellegrini, P. Orsini, E. Tognoni, C. Ascoli, P. Baschieri, and F. Dinelli, Pflug. Arch. Eur. J. Phys. **464**, 307 (2012).
[28]J. K. Zhang, M. Betson, J. Erasmus, K. Zeikos, M. Bailly, L. P. Cramer, and V. M. M. Braga, J. Cell Sci. **118**, 5549 (2005).
[29]A. E. Pelling, S. Sehati, E. B. Gralla, J. S. Valentine, and J. K. Gimzewski, Science **305**, 1147 (2004).
[30]A. E. Pelling, F. S. Veraitch, C. P. K. Chu, B. M. Nicholls, A. L. Hemsley, C. Mason, and M. A. Horton, J. Mol. Recognit. **20**, 467 (2007).